*Journal of the Nigerian Association of Mathematical Physics*
*Volume 56*(**March – May** *2020 Issue*), **pp185 – 190**


# PHASE TRANSFORMATIONS AND OPTICAL PROPERTIES OF Li-DOPED ZINC OXIDE: $Li_xZnO_{1-x}$ ($0.1 \leq x \leq 0.4$) AS A TRANSPARENT CONDUCTING OXIDE FOR OPTO-ELECTRONIC APPLICATIONS

*[1]M. Alpha, [2]A. Z. Ngari, [3]D. Jauro, [4]M. D. Abore and [5]M. H. Ibrahim*

*[1, 2]Department of Physics, Nigerian Army University Biu, P.M.B 1500.Borno State*
*[3] Department of Physics, University of Maiduguri, Borno State*
*[4] Department of Chemistry, Nigerian Army University Biu, Borno State*
*[5]Department of Physics, Federal University Gusau, Zamfara State, Nigeria.*

## *Abstract*

***The phase composition and structural transformations of Li-doped Zinc oxide: $Li_xZnO_{1-x}$ ($0.1 \leq x \leq 0.4$) was synthesised by solid state reaction technique. The sample was calcinated at 1073 K for 10 hours after which the pelletised samples were sintered at 1473 K for 10 hours to get homogenous samples. The DTA characterisation shows that for all the Li-doped samples, the phase transition is exothermic and there is no change in the phase of the samples below room temperature. A phase transition occurs at 375 K for the doped ZnO and increases as Li concentration increases with the highest phase transition temperature occurring at 396.4 K for $Li_{0.4}ZnO_{0.6}$ composite. The SEM images show that the doped $Li^+$ is sandwiched chemically within the layers of the zinc oxide, resulting into 3D architectural material and reveals good quality dispersion. The lateral grain size of the composites material shows an extensive distribution, ranging from 80 µm to 100 µm. The increase in the value of the optical band gap signifies a shift of the absorption towards a higher wavelength region. This also implies that increase in the doping of Li concentration increases the band gap energy required for the excitation charge carriers in network of the ZnO molecules.***

***Keywords*:** Zinc Oxide, Phase Transformation, Temperature and Optical Properties

## 1. Introduction

Zinc Oxide crystallite, among all other functional materials plays an outstanding role in terms of morphology, variety and also in terms of physical and chemical properties. Zinc oxide is of two main forms; hexagonal wurtzite and cubic zinc blende [1]. The wurtzite structure is most stable at ambient conditions and thus most common. The zinc blende form can be stabilised by growing ZnO on substrates with cubic lattice structure. In both cases, the zinc and oxide centres are tetrahedral, the most characteristic geometry for ZnO [2]. In addition to the wurtzite and zinc blende polymorphs, ZnO can be crystallised in the rock salt motif form at relatively high pressures [3]. The Hexagonal and zinc blende polymorphs have no inversion symmetry (reflection of a crystal relative to any given point does not transform it into itself). As in most group II-VI materials, the bonding in ZnO is largely ionic ($Zn^{2+}$ $O^{2-}$) with the corresponding radii of 0.074 nm for $Zn^{2+}$ and 0.140 nm for $O^{2-}$ This property accounts for the preferential formation of wurtzite rather than zinc blende structure [4], as well as the strong piezoelectricity of ZnO. Because of the polar Zn-O bonds, zinc and oxygen planes are electronically charged. To maintain electrical neutrality, planes reconstruct at atomic level in most materials, but not in $ZnO^-$ its surface is atomically flat, stable and exhibits no reconstruction [5].

ZnO nano crystalline materials have small size effect, quantum size effect, volume effect, surface effect and macroscopic quantum tunnel effect. It gives excellent characteristics in mechanics, catalysis, optics, electrics, magnetics, acoustics, calorific, superconducting technology, chemical activity. Recently ZnO has become a foundation for developing special materials and has been active in the fields of physical, chemical and materials science research [6, 7, 8]. In the continuous extensive research on ZnO nano crystallite, it has become especially important to obtain highly pure, super fine and uniform nano crystallite with possible physical, chemical and optical properties, and produce new nanomaterials. The key to unravelling the demand lies in the research and development of new synthesis techniques. The study on the solid-state chemical reaction under ambient temperature and near ambient temperature has made great progress in recent years. Solid-state chemical reaction to produce nanomaterials is a new technique which was developed recently. The synthesis of nano crystallite usually involves: clean surface, controllable particle shape, size distribution that inhibits particle agglomeration, easy collection, better stability and high productivity. The solid-state chemical reaction method can meet these needs and it is easy to operate with advantages of simple procedures such as synthesis, high yield, high selectivity, uniform particle size distribution, controllable size and less pollution. Li doped ZnO can prevent the occurrence of agglomeration of

Corresponding Author**:** Alpha M., Email: alphamatthew4@gmail.com, Tel: +2348062459364

the liquid phase and the phenomenon of particle agglomeration caused by intermediate step and high-temperature reaction [9, 10, 11]. The solid-state chemical reaction process comprises three steps: reaction, nucleation and growth. When the nucleation rate is greater than the nucleus's growth speed, it is helpful for the formation of nano crystallite. But if the nucleus's growing rate is greater than the nucleation rate, a lump crystal forms [12, 13]

Differential Thermal Analysis (DTA) is basically a technique for observing changes in energy level of a sample as a function of temperature. The changes were observed by providing a pair of thermocouples connected with electrical lead from their other ends, placing a sample substance near one of the thermocouples and a reference substance near the other, heating the sample substance and the reference substance at a programmed rate and observing the differential voltage developed by the pair of thermocouples. The voltage differential developed is proportional to the changes in energy level of the sample substance different from the changes in energy level of the reference substance [14]. Thermal matching between the sample and the reference is often improved by diluting the sample with the inert reference, keeping the total masses in each crucible as close to each other as possible.

## 2. Experiment

Solid state reaction technique in which polycrystalline solids were prepared from a mixture of solid starting materials and heated at high temperature was used for the synthesis of these compounds. The compounds (ZnO and $Li_2CO_3$) were synthesised for the following compositions; $Li_{0.1}ZnO_{0.9}$, $Li_{0.2}ZnO_{0.8}$, $Li_{0.3}ZnO_{0.7}$ and $Li_{0.4}ZnO_{0.6}$

### 2.1 Synthesis of Li Doped ZnO

All precursor chemicals used (ZnO and $Li_2CO_3$) in the synthesis were of analytical grade. The synthesis was carried out by solid state reaction technique. After the compositions have been weighted out using an analytical balance, they were placed in a petri dish and were mixed thoroughly using a spatula. 10mls of ethanol ($C_2H_5OH$) was added to the mixture to aid homogeneity. The paste formed was mixed thoroughly, during the process of grinding and mixing, the ethanol liquid gradually volatised and evaporated completely. The mixture was placed in a platinum crucible, placed in an RHF 1600 Carbonite England Furnace for Calcination at 1073 K for 10 hours. The obtained white powder was thoroughly grounded using an Agate Mortar and Pestle and then pressed into circular pellets of 19 mm in diameter and thickness of 4 mm using three (3) drops of toluene ($C_6H_5CH_3$) mixed with Polyvinyl Chloride (PVC) as the binder and applying pressure of about 20,000 pounds per square inch. The prepared pellets were then sintered at a temperature of 1473 K for 11 hours and furnace cooled in order to obtain a crystalline phase.

### 2.2 DTA Characterisation of Li Doped ZnO

The change in the energy level of the samples as a function of temperature was studied using Differential Thermal Analysis (DTA) technique. A NETZSCH DTA 404 PC with Pu 1,851.08 power unit was used from between 300 and 573 K at heating rate of 20 K/min and the result of the peak values for each sample was recorded for analysis.

### 2.3 Scanning electron microscopy (SEM) Characterisation

The surface morphology and microstructure of all samples in this work were investigated using Phenoworld Pro X Model scanning electron microscope (SEM) operated at 2 kV in secondary electron detection mode.

### 2.4 UV Characterisation

The optical transmittance and absorbance versus wavelength measurement were made using UV-1800 SHIMADZU, UV spectrophotometer at room temperature after which the optical band gap $E_g$ was estimated from the Tauc's plot.

## 3. Results and discussion

In the DTA characterisation from 300 to 573 K, below room temperature, there is no change in the phases of all the samples of doped ZnO as shown in Figure 1, in agreement with the work of [14]. The plots of $Li_{0.1}ZnO_{0.9}$ shows an anomaly which corresponds to a phase transition at a temperature of 375 K and it can be seen that the peak is very steep and narrow indicating a sharp change of phase. Since at this temperature, 375 K is far less than the melting point of ZnO which is 2248 K, it showed that the compound is not melting but there is a structural transformation going on at this temperature. As the doping concentration increases, the transition temperature increases as well, due to the grain size increases because of the Li doping. There is a difference in the transition temperature in this work and those of the previous reports which is as a result of the difference in the amount of Li concentration. There is a decrease in the phase transition temperature for $Li_{0.2}ZnO_{0.8}$, but then increases for $Li_{0.3}ZnO_{0.7}$ and $Li_{0.4}ZnO_{0.6}$ respectively. These decrease and increase could be as a result of Li attaining its solubility limit. As also shown in figure 1, it was observed that the transition is exothermic in which there is a release of energy in the form of heat as the structure transformed from hexagonal to another structure. The new structure was unstable, and immediately at 375 K an endothermic reaction occurred in which the sample absorbed energy to gain stability by quickly transforming into a stable structure. In its new structure and immediately at a temperature of 378 K after it has stabilized, an exothermic reaction occurred. As shown in Figure 1, the transition is exothermic for all the Li doped ZnO samples.

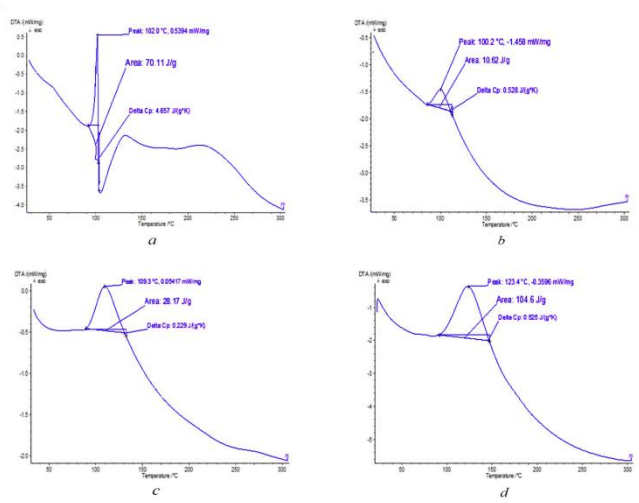


Figure 1 DTA Plots of Li $_x$ZnO$_{1-x}$ (0.10 ≤X≤ 0.40) samples from 300 to 573 K (a) of Li $_{0.1}$ZnO$_{0.9}$ (b) Li$_{0.2}$ZnO$_{0.8}$ (c) Li $_{0.3}$ZnO$_{0.7}$ (d) Li $_{0.4}$ZnO$_{0.6}$

**Table 1 Temperature of the phase transition of Li$_x$ZnO$_{1-x}$ (x = 0.10 to 0.40)**

| Samples | Temperature of Phase Transition (K) | Temperature of Phase Transition ($^0$C) |
|---|---|---|
| Li$_{0.1}$ZnO$_{0.9}$ | 375.0 | 102.0 |
| Li$_{0.2}$ZnO$_{0.8}$ | 373.2 | 100.2 |
| Li$_{0.3}$ZnO$_{0.7}$ | 382.3 | 109.3 |
| Li$_{0.4}$ZnO$_{0.6}$ | 396.4 | 123.4 |

It was also observed from Figure 1 that the peaks of the Li doped ZnO samples at the transition temperature are broad for (x = 0.20 to 0.40). This indicates that the phase transition is not occurring at once but occurs gradually over a range of temperature in the doped ZnO samples. This is as a result of Li atoms occupying off-centred positions, in which the order-disorder characteristics can be direct or phonon-mediated between off-centred Li ions and displaced characteristics relating to translational shifts of Zn and O sub-lattices having effect on the phase transition. This leads to a dielectric anomaly which increases as the phase transition increases

The SEM images are given in figure 2 and the XRF spectra in figure 3. The XRF spectra give the chemical composition of the composite material while the SEM images in figure 2 indicated that, there was a slight increase in the number of grain boundaries, signifying a breakdown of the surface coalescence with increasing dopant concentration. However, since all the samples were synthesis under identical conditions, an almost similar microstructure and surface morphology was seen in all the doped composites irrespective of the doping concentration. The increase in doping concentration improves accessibility due to their metal-cation and regular 3D dispersion of $Li^+$ in the structure of the ZnO. The SEM images show that the doped $Li^+$ is sandwiched chemically within the layers of the zinc oxide, resulting into 3D architecture material and reveals good quality dispersion. The lateral grain size of the composites material exhibits a wide distribution up to 100 µm.

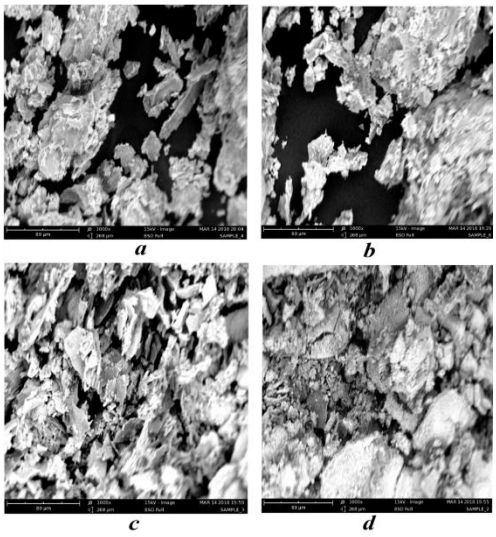


Figure 2 SEM Images showing morphology for (a) Li $_{0.1}$ZnO$_{0.9}$ (b) Li $_{0.2}$ZnO$_{0.8}$ (c) Li $_{0.3}$ZnO$_{0.7}$ (d) Li$_{0.4}$ZnO$_{0.6}$

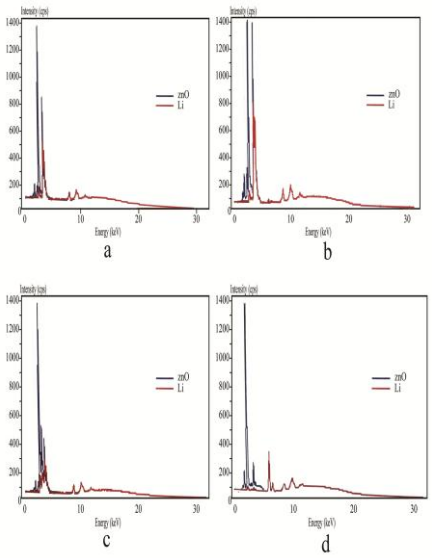


Figure 3 XRF Spectra for (a) Li $_{0.1}ZnO_{0.9}$ (b) Li $_{0.2}ZnO_{0.8}$ (c) Li $_{0.3}ZnO_{0.7}$ (d) Li $_{0.4}ZnO_{0.6}$

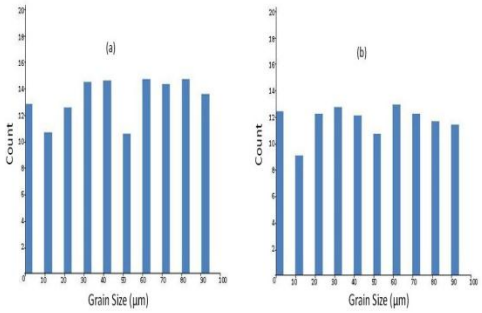


Figure 4 Grain size distributions from SEM images for (a) $Li_{0.1}ZnO_{0.9}$ (b) $Li_{0.2}ZnO_{0.8}$

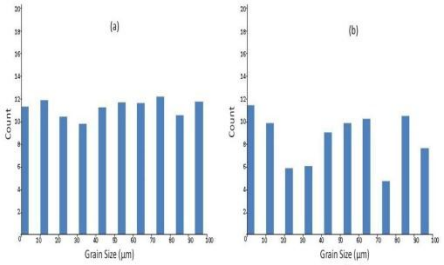


Figure 5 Grain size distributions from SEM images for (a) $Li_{0.3}ZnO_{0.7}$ (b) $Li_{0.4}ZnO_{0.6}$

From grain size distributions of the SEM images obtained using ImageJ software, the lateral grain size of the Li doped ZnO exhibits a wide and non-uniform distribution as shown in the Figures (4 and 5), ranging from 0 to 100 μm. It is also clearly seen from Figures (4 and 5) that the grain size for the composite are closely packed. This can be attributed the increase in the electron density in the conduction band due the introduction of the active $Li^+$ into the network zinc oxide. From the Figures (4 and 5), the preferred grain distributions occur between (20 - 90) μm. These wide grain distributions observed from the composites could be link to the preferred crystal orientation in the materials caused by defects as a result of the presence of the $Li^+$ in the network of the ZnO.

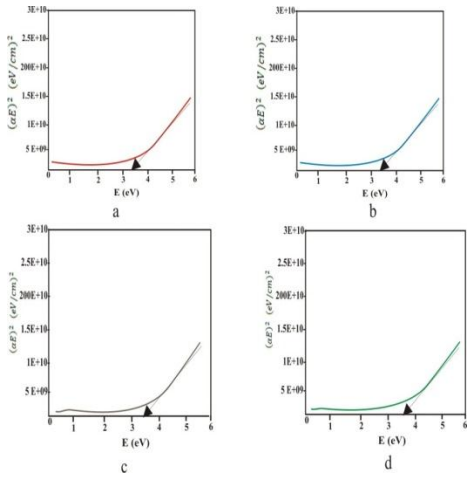


Figure 6 Tauc's plot for (a) Li $_{0.1}ZnO_{0.9}$ (b) Li $_{0.2}ZnO_{0.8}$ (c) Li $_{0.3}ZnO_{0.7}$ (d) Li $_{0.4}ZnO_{0.6}$

The optical bang gap was estimated by extrapolation of the Tauc's plot as shown in figure 6. The composites $Li_{0.1}ZnO_{0.9}$ give an estimated optical band gap of 3.1 eV, $Li_{0.2}ZnO_{0.8}$ give an estimated band gap of 3.2 eV, $Li_{0.3}ZnO_{0.7}$ gives 3.4 eV and $Li_{0.4}ZnO_{0.6}$ gives 3.6 eV. The increase in the value of the optical band gap signifies a shift of the absorption towards the higher wavelength region. This also implies that increase in the doping of Li concentration increases the band gap energy required for the excitation charge carriers in network of the ZnO molecules.

## 4. Conclusion

In conclusion, the DTA characterisation shows that for all the Li-doped samples, the phase transition is exothermic and there is no change in phase of the samples below room temperature. A phase transition occurs at 375 K for the doped ZnO and increases as Li concentration increases with the highest phase transition temperature occurring at 396.4 K for $Li_{0.4}ZnO_{0.6}$ sample. The SEM images show that the doped $Li^+$ is sandwiched chemically within the layers of the zinc oxide, resulting into 3D architectural material and reveals good quality dispersion. The lateral grain size of the composites material exhibits a wide distribution of up to 100 µm. The increase in the value of the optical band gap signifies a shift of the absorption towards the higher wavelength region. This also implies that increase in the doping of Li concentration increases the band gap energy required for the excitation charge carriers in network of the ZnO molecules.

## REFERENCES

[1] Bai, C., Liu, M. (2013). From chemistry to nanoscience: not just a matter of size. *International Edition* 52(10), 2678.

[2] Baruah, S., Dutta, J. (2009). Hydrothermal Growth of ZnO Nanostructures. *Journal of Sci. Technol. Adv. Mater*, 10, 130-137.

[3] Klingshirn, C. F., Bruno, K.M., Andreas,W., Axel, H., Johannes,M.M.G. (2010). Zinc Oxide: From Fundamental Properties. *Towards Novel Applications*. ISBN 978.3-642-10576.

[4] Ma, J.Q., Shen, Y. (2014). Al-doping Chitosan-Fe (Ⅲ) hydrogel for removal of fluoride from Aqueous solutions, *Chemical Engineering Journal*, 248, 98-112.

[5] Nicholson, J.W. (1998). The chemistry of cements formed between zinc oxide and aqueous Zinc Chloride. *Journal of Material Science*, 33 (9), 2251, doi:10.1023/a.1004327018497

[6] Nikolay, K., Jorge, G., Freek. (2016). Recent developments in zeolite membranes for gas Separation. *Journal of Membrane Science* 499, 65-73.

[7] Qiang, J.B., Wang, Y. M., Wang, D. H. (2004). Quasicrystals in the Ti-Zr-Ni Alloy Systerm. *J. Non-Cry. Sol*., 334(335), 223-229.

[8] Ozgur, U., Alivov, Y.L., Liu, C., Teke, A., Reshchikov,M.A., Dogan, S., Avrutin,V. (2005). A Comprehensive review of ZnO materials and device. Journal of Applied Physics 98 (4), 123-130: 041301, doi: 10.1063/1.1992666

[9] Si, W.Y., Pei, X.M., Jia, H S. (2005). Preparation of Nanosized $Al_2O_3$. *Diamond and Abrasives Engineering*, 146, 33-41.

[10] Tong,W P., Tao, N. R., Wang Z B. (2003). Nitriding Iron at Lower Temperatures, *Science*, 299, 686-692.

[11] Wang, X.S., Wu, Z.C., Webb, J.F., Liu, Z.G. (2003). Ferroelectric and dielectric Properties of Li-doped ZnO thin films prepared by pulsed laser deposition. *Journal of applied physics A*, 77, 561-565, doi: 10.1007/S00339-002-1497

[12] Wang, Y., 2004. Nano and Submicron-structured Sulphide Self-lubricating Coatings, *Tribology Letters*, 17(2) 165.

[13] Zhao, X., Huang, L., Li, H. R. (2016). Promotional effects of zirconium doped $CeVO_4$ or the low-temperature selective catalytic reduction of NOx with NH3, *Applied Catalysis B: Environmental*, 183, 269-277.

[14] Zhuang, J., Chi Y. H., Wang D. (2008). Preparation of Different Topography $NiCo_2O_4$ with Surfactant by Solid State Reaction, *Journal of Inorganic Materials*, 22(1), 40-49.